Experimental test of the trade-off relation for quantum coherence

Wei-Min Lv, Chao Zhang,* Xiao-Min Hu, Huan Cao, Jian Wang, Yun-Feng Huang,†
Bi-Heng Liu, Chuan-Feng Li,‡ and Guang-Can Guo
CAS Key Laboratory of Quantum Information, University of Science and Technology of China, Hefei 230026, People's Republic of China and CAS Center For Excellence in Quantum Information and Quantum Physics, University of Science and Technology of China, Hefei 230026, People's Republic of China

(Received 13 August 2018; published 28 December 2018)

As one of the most essential properties of quantum mechanics, quantum coherence is also considered a key physical resource which can be used to accomplish certain tasks of quantum information processing. Significant efforts are involved in the quantification of quantum coherence using measures such as the l_1-norm and the relative entropy of coherence. The quantum coherence as a physical resource is usually defined with respect to a given basis, which also arouses an issue of interest concerning the variation of quantum coherence for a quantum state in different reference bases. In this paper, using an all optical setup, we experimentally investigate a trade-off relation between the coherence measures quantified by relative entropy of coherence in two noncommuting reference bases. Our result shows that the sum of quantum coherence under these bases is bounded in a region defined by its lower bound and upper bound.

DOI: 10.1103/PhysRevA.98.062337

I. INTRODUCTION

Originating from the superposition principle of quantum states, quantum coherence, like the uncertainty principle, is one of the most fundamental features of quantum mechanics that distinguishes it from the classical realm. There are increasing research efforts leading quantum coherence to be considered a fundamental resource in the applications of quantum information processing [1–7], quantum thermodynamics [8–10], and quantum metrology [11–15], as a "a measure of the strength of quantum correlations [16]." Although the studies of quantum coherence have a long-standing history [5,17–21], the coherence in the framework of resource theories has been rigorously characterized only recently [22,23], resulting in quantifications of coherence such as the l_1-norm, relative entropy, and skew information that are related to both the quantum states and the corresponding reference bases. Since the measurements of coherence are basis dependent, the relationship between the amounts of coherence for a quantum state in different bases is an issue of interest.

Recently, a trade-off relation for the coherence of a bipartite state ρ_{AB} defined in two different reference bases was derived by Singh *et al.* [24]; it can be termed an uncertainty relation in which the uncertainty is quantified by the relative entropy of coherence in the given bases. The uncertainty relation for the quantum coherence is given by

$$C^{(r\mu)}(\rho_{AB}) + C^{(s\mu)}(\rho_{AB}) \geqslant \log_2 \frac{1}{c} - S(A|B) + \max\{0, \mathcal{D} - \mathcal{J}\}, \quad (1)$$

where A and B represent the subsystems of the bipartite state ρ_{AB} respectively, and $C^{(x\mu)}(\rho_{AB}) = S(\rho_{XU}) - S(\rho_{AB})$ is the relative entropy of coherence. $\rho_{XU} = \sum_{x,\mu} p_{x,\mu}|x\rangle\langle x| \otimes |\mu\rangle\langle\mu|$ denotes the state that can be considered as the diagonal part of the density matrix ρ_{AB} represented in the bases $\{|x\rangle \otimes |\mu\rangle\}$, with $p_{x,\mu} = \langle x, \mu|\rho_{AB}|x, \mu\rangle$, $\{|\mu\rangle\}$ are the eigenvectors of the reduced density matrix ρ_B of the system state ρ_{AB}, $\{|x\rangle\}$ are the eigenvectors of the observable X, and $\{|r\rangle\}$ and $\{|s\rangle\}$ are also the eigenvectors of the observable X as $X = R$ and $X = S$, respectively. For right-hand side of inequality (1), $c = \max_{r_i,s_j} |\langle r_i|\, s_j\rangle|^2$, the conditional entropy $S(A|B) = S(\rho_{AB}) - S(\rho_B)$, and the lower bound can be tighten when $\mathcal{D} - \mathcal{J} > 0$, where $\mathcal{D}$ is the quantum discord across the AB partition and $\mathcal{J}$ is the classical correlation [25–28], which is defined by $\mathcal{J} = \max_{\{|u\rangle\langle u|\}}[S(\rho_U) + S(\rho_B) - S(\rho_{UB})]$, with $\rho_{UB} = \sum_u |u\rangle\langle u| \otimes \mathrm{Tr}_A[(|u\rangle\langle u| \otimes I)\rho_{AB}]$, and the optimization takes over all the positive-operator valued measures (POVMs) $\{|u\rangle\langle u|\}$ acting on the subsystem A.

Besides, the left-hand side of inequality (1) is also upper bounded by

$$C^{(r\mu)}(\rho_{AB}) + C^{(s\mu)}(\rho_{AB}) \leqslant 2\log_2 d_A - 2S(A|B), \quad (2)$$

where d_A is the dimension of the subsystem A of ρ_{AB}.

In this paper, we report an all-optical experimental investigation of the trade-off relation between the coherence measures in two different reference bases. Our experimental results show that the quantum coherence measures of a bipartite quantum system in two incompatible bases are not reciprocally independent, which means that if the coherence of the state measured in one basis shows a larger value, it would not give the same value in another base. What is more, we find an interesting phenomenon that the lower bound in inequality (1), that is restricted by the uncertainty relation for coherence, would not be tightened with the presence of

*zhc1989@ustc.edu.cn
†hyf@ustc.edu.cn
‡cfli@ustc.edu.cn

entanglement, which behaves in the opposite way compared to the entropic uncertainty relation [29–32].

II. EXPERIMENT

In the following, we report our experimental results from studying the trade-off relation for quantum coherence, where the experimental setup is shown in Fig. 1. To investigate inequalities (1) and (2), in principle one should check through all possible bipartite quantum states, which is not practical for real experiments. So we choose to adopt the most popularly used class of bipartite quantum state here. In our experiment, the Werner states are considered to be the most suitable candidate states [33]. For our photon-polarization-qubit system, the Werner state can be expressed as

$$\rho_W = p|\psi^-\rangle\langle\psi^-| + \frac{1-p}{4}\boldsymbol{I}, \tag{3}$$

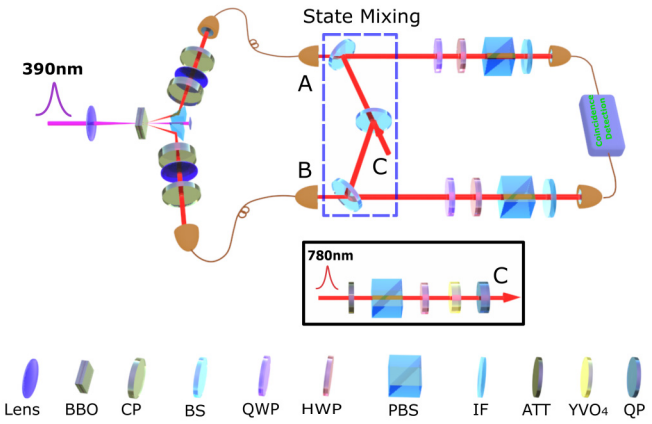

FIG. 1. Experimental setup. A pair of polarization-entangled photons A and B with the state $\frac{1}{\sqrt{2}}(|HV\rangle - |VH\rangle)$ is generated by a spontaneous parametric down-conversion (SPDC) process, i.e., a 390-nm pulse, produced by a frequency doubling process of an ultrafast pulse (780-nm central wavelength, 76-MHz repetition rate, 140-fs duration) from a mode-locked Ti:sapphire laser, passes through a sandwich-like BBO crystal to create the polarization-entangled photons A and B. The blue dotted box represents the mixing process in which the two entangled photons A and B, through the two beam splitters (BSs), are combined with the strongly attenuated and completely depolarized photons C, which are generated via a decoherence process shown in the inset (black line box); i.e., a 780-nm pulse is attenuated to a weak coherent state with only a very small probability (∼0.005) of containing a single photon in each pulse by using an attenuator (ATT), a polarization beam splitter (PBS), and a half-wave plate (HWP) with its angle set to 22.5°, and then the attenuated pulse passes through a 1.21-mm yttrium orthovanadate (YVO_4) crystal and 400λ (780-nm) quartz plate (QP) to be completely decohered before being split into two spatial modes. Using the ATT to change the intensity of photon C, the desired Werner states can be prepared by controlling the ratio between the entangled photons and decohered photons. For state measurement, the photons A and B are sent to the polarization analysis measurement device which contains a quarter-wave plate (QWP), a HWP, and PBS before passing through the 3-nm interference filter (IF). By changing the angles of the QWPs and HWPs, the density matrix of the characterized target state can be reconstructed.

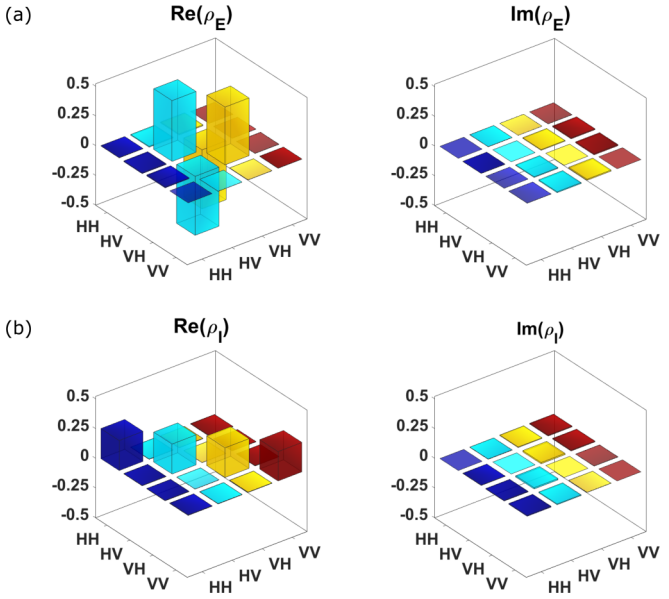

FIG. 2. Tomographic reconstructed matrices of the prepared maximally entangled state $|\psi^-\rangle$ and the identity state $\boldsymbol{I}$. (a) Re(ρ_E) and Im(ρ_E) represent the real and imaginary parts of $|\psi^-\rangle$ respectively. (b) Re(ρ_I) and Im(ρ_I) represent the real and imaginary parts of $\boldsymbol{I}$ respectively.

where $0 \leqslant p \leqslant 1$ and $|\psi^-\rangle = \frac{1}{\sqrt{2}}(|HV\rangle - |VH\rangle)$, with H and V representing the polarization of entangled photons. $\boldsymbol{I} = \mathrm{diag}[1, 1, 1, 1]$ denotes the identity state. On the one hand, it has a certain degree of universality that can vary from maximally mixed state to maximally entangled state, which motivates many efforts numerically and experimentally on the research of quantum correlation [34–37]. On the other hand, for Werner states, $\{|\mu\rangle\}$ are always the eigenvectors of the observable σ_z that make it possible to readily measure the state ρ_{XU}, which originates from the Werner states $\rho_{AB} = \rho_W$ after the projective measurements by $\{|x\rangle\langle x| \otimes |\mu\rangle\langle\mu|\}$.

According to Eq. (3), the preparation of the Werner states requires the mixture of the entangled state $|\psi^-\rangle$ with the identity state $\boldsymbol{I}$, which can be seen in Fig. 1. The entangled state $|\psi^-\rangle$ is prepared via the spontaneous parametric down-conversion (SPDC) process that generates a pair of polarization-entangled photons, A and B, with maximally entangled state $\frac{1}{\sqrt{2}}(|HV\rangle - |VH\rangle)$ [38]. The identity state $\boldsymbol{I}$ is prepared via a decoherence process, in which the strongly attenuated 780-nm pulse, in polarization state $\frac{1}{\sqrt{2}}(|H\rangle + |V\rangle)$, is completely depolarized by using a 1.21-mm yttrium orthovanadate (YVO_4) crystal (corresponding to about 340λ quartz plate) and 400λ (780-nm) quartz plate (QP), which amounts to about a 740λ (780-nm) quartz plate, to entangle the polarization and frequency degree of the photons; then the latter will be traced out in the measurement setup, such that it equals an identity state in the polarization degree of freedom. The entangled state $|\psi^-\rangle$ and the identity state $\boldsymbol{I}$ were both prepared with rather high fidelity, $F = 0.9946 \pm 0.0004$ and $F = 0.9996 \pm 0.0001$, respectively, and the error bars are estimated according to the Monte Carlo method [39]. Figure 2 shows the real and imaginary parts of $|\psi^-\rangle$ and

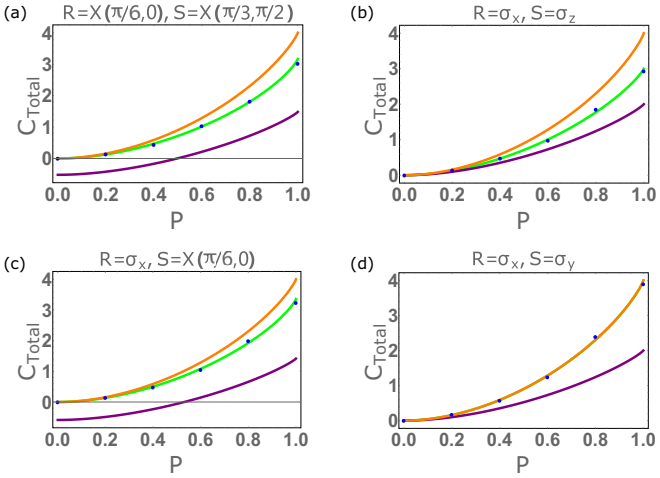

FIG. 3. Experimental results and theoretical predictions for the input Werner states ρ_W: The x axis represents the different Werner states, which are determined by the parameter p. The y axis represent the values of the corresponding terms of interest, and $C_{\text{Total}} = C^{(r\mu)}(\rho_W) + C^{(s\mu)}(\rho_W)$ denotes the coherence measured in two different bases. The blue circles represent the experimental results for C_{Total}, and the green solid line represents its theoretical prediction, while the purple and orange solid lines represent the theoretical predictions of the lower bound $\log_2 \frac{1}{c} - S(A|B) + max\{0, \mathcal{D} - \mathcal{J}\}$ and the upper bound $2\log_2 d_A - 2S(A|B)$, respectively. (a) shows the experimental results and theoretical predictions of the coherence, lower bound, and upper bound in a general case where the observables $R = X(\frac{\pi}{6}, 0)$, $S = X(\frac{\pi}{3}, \frac{\pi}{2})$. (b)–(d) show the special cases where $R = \sigma_x$, $S = \sigma_z$; $R = \sigma_x$, $S = X(\frac{\pi}{6}, 0)$; and $R = \sigma_x$, $S = \sigma_y$, respectively.

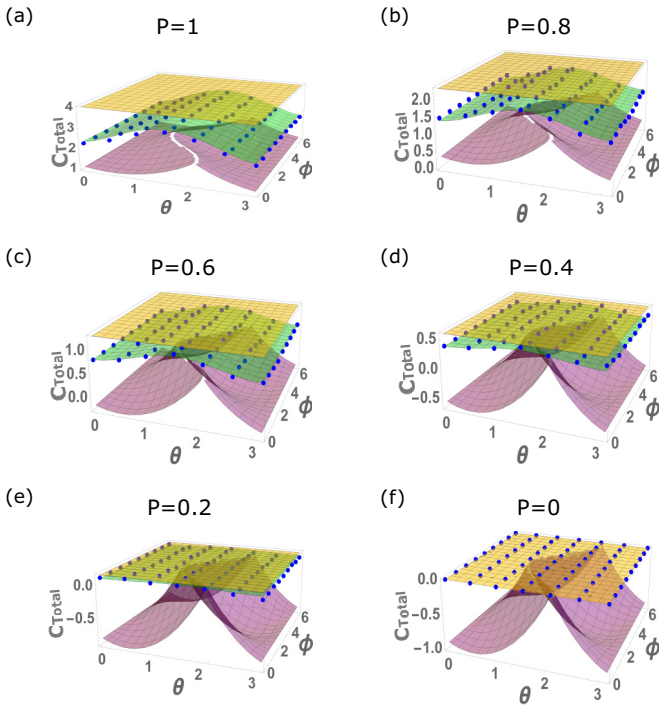

FIG. 4. Experimental results and theoretical predictions for the input Werner states ρ_W in the case where $R = X(\frac{\pi}{6}, 0)$ and S is a function of the parameters θ and ϕ (θ and ϕ are in units of radians): The blue circles represent the experimental results for $C^{(r\mu)}(\rho_W) + C^{(s\mu)}(\rho_W)$ and the green surface represents its theoretical prediction, while the purple and orange surfaces represent the theoretical predictions of the lower bound $\log_2 \frac{1}{c} - S(A|B) + \max\{0, \mathcal{D} - \mathcal{J}\}$ and the upper bound $2\log_2 d_A - 2S(A|B)$, respectively. (a)–(f) show the experimental results and theoretical predictions of the coherence, lower bound, and upper bound for Werner states with different parameters p, respectively.

$\boldsymbol{I}$. Distinguishing from the time-mixing technique [35,36,40], we spatially combine these two modes with the two entangled-photon modes of A and B respectively. In this way, a series of Werner states with different p can be prepared by controlling the ratio between the entangled state $|\psi^-\rangle$ and the identity state $\boldsymbol{I}$.

Next, to evaluate the left-hand sides of inequalities (1) and (2), the two photons prepared in the Werner state are both sent to the polarization analysis measurement device before passing through 3-nm bandwith interference filters (IFs). By changing the angles of the QWPs and HWPs, one can reconstruct not only the density matrix ρ_W of the prepared states [41] but also that of the state ρ_{XU}, which can be measured directly. To achieve this, we measure photon B in the eigenbasis of the observable σ_z, and simultaneously measure photon A in the observable X's eigenbasis. After normalization, the measured coincidence counts correspond to the elements in ρ_{XU} directly. Therefore, the coherence $C^{(x\mu)}(\rho_W) = S(\rho_{XU}) - S(\rho_W)$ in the reference basis $\{|x\rangle\langle x| \otimes |\mu\rangle\langle\mu|\}$ can be obtained with the reconstructed density matrix ρ_W and the measured ρ_{XU}. At last, the right-hand sides of inequalities (1) and (2) can be evaluated by theoretically calculating the conditional entropy $S(A|B)$, the corresponding quantum discord $\mathcal{D}$, and classical correlation $\mathcal{D}$ using the density matrix of the ideal target Werner state [42,43].

The experimental results and theoretical predictions for the coherence $C^{(r\mu)}(\rho_W) + C^{(s\mu)}(\rho_W)$, the lower bound $\log_2 \frac{1}{c} - S(A|B) + \max\{0, \mathcal{D} - \mathcal{J}\}$, and the upper bound $2\log_2 d_A - 2S(A|B)$ are shown in Fig. 3. $C^{(r\mu)}(\rho_W)$ is the coherence characterized in the basis $\{|r\rangle\langle r| \otimes |\mu\rangle\langle\mu|\}$, where $\{|r\rangle\}$ is the eigenvector of the observable $X = R$ and $C^{(s\mu)}(\rho_W)$ is similar for $X = S$, with $X = \hat{n} \cdot \vec{\sigma}$, $\hat{n} = \{\sin\theta\cos\phi, \sin\theta\sin\phi, \cos\theta\}$, and $\vec{\sigma} = \{\sigma_x, \sigma_y, \sigma_z\}$ are the Pauli matrices. With the increase of the parameter p in the x axis, the Werner state changes from the maximally mixed state $\boldsymbol{I}$ to the maximally entangled state $|\psi^-\rangle$. Figure 3(a) shows the experimental results and theoretical predictions in the case where the observables $R = X(\frac{\pi}{6}, 0)$ and $S = X(\frac{\pi}{3}, \frac{\pi}{2})$. A more general case with $R = X(\frac{\pi}{6}, 0)$, and the observable S being the function of θ and ϕ, can be seen in the Appendix. Figures 3(b)–3(d) correspond to the special cases where the observable $R = \sigma_x$, and S varies from σ_z to σ_y, which results in the coherence approaching to the upper bound. Panel (d) shows that the theoretical predictions of coherence overlap with its upper bound completely, and our experimental data points all coincide with the solid line of the upper bound, which also confirms that for the inequality (2) the equality holds when $R = \sigma_x$ and $S = \sigma_y$. Otherwise, the equality would hold only at a point where the parameter $p = 0$, which means the system state is a maximally mixed

state. It can be seen that our experimental results coincide with the theoretical predictions very well, which shows that the coherence measured in two different bases is always restricted in a region defined by the lower bound and the upper bound.

III. CONCLUSIONS

In the paper, with high fidelity of preparation of the Werner states, we have performed an experiment to investigate the trade-off relation between the coherence measures in the two noncommuting reference bases, which shows the quantum coherence characterized in one base is not independent of the other. The upper bound can fairly estimate the capacity of a quantum state as a quantum source in different bases, which can be used to accomplish the tasks that are otherwise impossible in classical physics. The lower bound respects the uncertainty relation (1), with the uncertainty quantified by quantum coherence, showing that the uncertainty measured in a basis is equivalent to the coherence measured in the same basis [44,45]. And when the quantum discord of the state is larger than its classical correlation, the lower bound uncertainty relation can be tighter.

Furthermore, we also find an interesting phenomenon that the gap between the uncertainty quantified by the coherence in two noncommuting bases and the lower bound would be larger with the increase of entanglement of the state. The origin of the uncertainty characterized in terms of entropy can be divided into two parts, the classical noise and quantum effect, and the former can be reduced by introducing entanglement with an ancillary system, such as quantum memory, while the quantum effect cannot [44–46]. The uncertainty quantified by coherence only originates from the quantum effect, which would not be reduced with the increase of the correlation of the states. We consider that it is the reason why the uncertainty relation (1) shows contrary behavior compared with the entropic uncertainty relation. Our work may be helpful for further understanding and study of the uncertainty principle and quantum coherence.

ACKNOWLEDGMENTS

This work was supported by the National Key Research and Development Program of China (Grant No. 2017YFA0304100) , the National Natural Science Foundation of China (Grants No. 61327901, No. 61490711, No. 11774335, No. 61225025, No. 11474268, No. 11374288, No. 11304305, and No. 11404319), the Key Research Program of Frontier Sciences, CAS (Grant No. QYZDY-SSW-SLH003), the National Program for Support of Top-notch Young Professionals (Grant No. BB2470000005), and the Fundamental Research Funds for the Central Universities (Grants No. WK2470000018 and No. WK2470000026).

APPENDIX

Figure 4 shows the experimental results and theoretical predictions for the coherence $C^{(r\mu)}(\rho_W) + C^{(s\mu)}(\rho_W)$, the lower bound $\log_2 \frac{1}{c} - S(A|B) + \max\{0, \mathcal{D} - \mathcal{J}\}$, and the upper bound $2\log_2 d_A - 2S(A|B)$, in a more general case with the observables R being fixed, and S varying.

[1] M. A. Nielsen and I. L. Chuang, *Quantum Computation and Quantum Information* (Cambridge University Press, Cambridge, UK, 2000).
[2] N. Gisin, G. Ribordy, W. Tittel, and H. Zbinden, Rev. Mod. Phys. **74**, 145 (2002).
[3] K. Bu, A. Kumar, and J. Wu, arXiv:1603.06322 (2016).
[4] X. Hu and H. Fan, Sci. Rep. **6**, 34380 (2016).
[5] A. Streltsov, G. Adesso, and M. B. Plenio, Rev. Mod. Phys. **89**, 041003 (2017).
[6] D. Mondal, T. Pramanik, and A. K. Pati, Phys. Rev. A **95**, 010301 (2017).
[7] D. Girolami and B. Yadin, Entropy **19**, 124 (2017).
[8] F. G. S. L. Brandão, M. Horodecki, J. Oppenheim, J. M. Renes, and R. W. Spekkens, Phys. Rev. Lett. **111**, 250404 (2013).
[9] M. Lostaglio, K. Korzekwa, D. Jennings, and T. Rudolph, Phys. Rev. X **5**, 021001 (2015).
[10] M. Lostaglio, D. Jennings, and T. Rudolph, Nat. Commun. **6**, 6383 (2015).
[11] S. L. Braunstein and C. M. Caves, Phys. Rev. Lett. **72**, 3439 (1994).
[12] V. Giovannetti, S. Lloyd, and L. Maccone, Nat. Photon. **5**, 222 (2011).
[13] I. Marvian and R. W. Spekkens, Phys. Rev. A **94**, 052324 (2016).
[14] D. Braun, G. Adesso, F. Benatti, R. Floreanini, U. Marzolino, M. W. Mitchell, and S. Pirandola, Rev. Mod. Phys. **90**, 035006 (2018).
[15] P. Giorda and M. Allegra, J. Phys. A: Math. **51**, 025302 (2018).
[16] O. Dannenberg, Ann. Phys. (Berlin) **17**, 355 (2008).
[17] R. J. Glauber, Phys. Rev. **131**, 2766 (1963).
[18] E. C. G. Sudarshan, Phys. Rev. Lett. **10**, 277 (1963).
[19] A. Albrecht, J. Mod. Opt. **41**, 2467 (1994).
[20] L. Mandel and E. Wolf, *Optical Coherence and Quantum Optics* (Cambridge University Press, Cambridge, UK, 1995).
[21] Y. Yao, X. Xiao, L. Ge, and C. P. Sun, Phys. Rev. A **92**, 022112 (2015).
[22] G. Gour and R. W. Spekkens, New J. Phys. **10**, 033023 (2008).
[23] T. Baumgratz, M. Cramer, and M. B. Plenio, Phys. Rev. Lett. **113**, 140401 (2014).
[24] U. Singh, A. K. Pati, and M. N. Bera, Mathematics **4**, 47 (2016).
[25] L. Henderson and V. Vedral, J. Phys. A: Math. Gen. **34**, 6899 (2001).
[26] H. Ollivier and W. H. Zurek, Phys. Rev. Lett. **88**, 017901 (2001).
[27] K. Modi, A. Brodutch, H. Cable, T. Paterek, and V. Vedral, Rev. Mod. Phys. **84**, 1655 (2012).
[28] A. K. Pati, M. M. Wilde, A. R. U. Devi, A. K. Rajagopal, and Sudha, Phys. Rev. A **86**, 042105 (2012).
[29] M. Berta, M. Christandl, R. Colbeck, J. M. Renes, and R. Renner, Nat. Phys. **6**, 659 (2010).
[30] R. Prevedel, D. R. Hamel, R. Colbeck, K. Fisher, and K. J. Resch, Nat. Phys. **7**, 757 (2011).
[31] C. F. Li, J. S. Xu, X. Y. Xu, K. Li, and G.-C. Guo, Nat. Phys. **7**, 752 (2011).

[32] P. J. Coles, M. Berta, M. Tomamichel, and S. Wehner, Rev. Mod. Phys. **89**, 015002 (2017).
[33] R. F. Werner, Phys. Rev. A **40**, 4277 (1989).
[34] Y. S. Zhang, Y. F. Huang, C. F. Li, and G. C. Guo, Phys. Rev. A **66**, 062315 (2002).
[35] B. Dakic *et al.*, Nat. Phys. **8**, 666 (2012).
[36] D. J. Saunders, A. J. Bennet, C. Branciard, and G. J. Pryde, Sci. Adv. **3**, e1602743 (2017).
[37] A. Orieux, M. Kaplan, V. Venuti, T. Pramanik, I. Zaquine, and E. Diamanti, J. Opt. **20**, 044006 (2018).
[38] C. Zhang, Y.-F. Huang, Z. Wang, B.-H. Liu, C.-F. Li, and G.-C. Guo, Phys. Rev. Lett. **115**, 260402 (2015).
[39] J. B. Altepeter, E. R. Jeffrey, and P. G. Kwiat, Adv. At. Mol. Opt. Phys. **52**, 105 (2005).
[40] J. Gao, L. F. Qiao, Z. Q. Jiao, Y. C. Ma, C. Q. Hu, R. J. Ren, A. L. Yang, H. Tang, M. H. Yung, and X. M. Jin, Phys. Rev. Lett. **120**, 240501 (2018).
[41] D. F. V. James, P. G. Kwiat, W. J. Munro, and A. G. White, Phys. Rev. A **64**, 052312 (2001).
[42] S. Luo, Phys. Rev. A **77**, 042303 (2008).
[43] M. Ali, A. R. P. Rau, and G. Alber, Phys. Rev. A **81**, 042105 (2010).
[44] X. Yuan, H. Zhou, Z. Cao, and X. F. Ma, Phys. Rev. A **92**, 022124 (2015).
[45] X. Yuan, Q. Zhao, D. Girolami, and X. F. Ma, arXiv:1605.07818.
[46] X. Yuan, G. Bai, T. Y. Peng, and X. F. Ma, Phys. Rev. A **96**, 032313 (2017).